On the calculation of complete dissociation curves of closed-shell pseudo-onedimensional systems via the complete active space method of increments

E. Fertitta, B. Paulus, G. Barcza, and Ö. Legeza

Articles you may be interested in

First-principles investigation of the dissociation and coupling of methane on small copper clusters: Interplay of collision dynamics and geometric and electronic effects
J. Chem. Phys. **142**, 184308 (2015); 10.1063/1.4919948

Active-space coupled-cluster study of electronic states of Be 3
J. Chem. Phys. **123**, 074319 (2005); 10.1063/1.2001656

Evolution of the electronic structure of Be clusters
J. Chem. Phys. **123**, 074329 (2005); 10.1063/1.2001655

Ab initio calculations for the photoelectron spectra of vanadium clusters
J. Chem. Phys. **121**, 5893 (2004); 10.1063/1.1785142

Quantum chemistry using the density matrix renormalization group II
J. Chem. Phys. **119**, 4148 (2003); 10.1063/1.1593627

On the calculation of complete dissociation curves of closed-shell pseudo-onedimensional systems via the complete active space method of increments

E. Fertitta,[1] B. Paulus,[1] G. Barcza,[2] and Ö. Legeza[2]

[1]*Institut für Chemie und Biochemie, Freie Universität Berlin, Takustr. 3, 14195 Berlin, Germany*
[2]*Strongly Correlated Systems "Lendület" Research Group, Wigner Research Centre for Physics, P.O. Box 49, Budapest, Hungary*

The method of increments (MoI) has been employed using the complete active space formalism in order to calculate the dissociation curve of beryllium ring-shaped clusters Be_n of different sizes. Benchmarks obtained through different quantum chemical methods including the *ab initio* density matrix renormalization group were used to verify the validity of the MoI truncation which showed a reliable behavior for the whole dissociation curve. Moreover we investigated the size dependence of the correlation energy at different interatomic distances in order to extrapolate the values for the periodic chain and to discuss the transition from a metal-like to an insulator-like behavior of the wave function through quantum chemical considerations. © *2015 AIP Publishing LLC.* [http://dx.doi.org/10.1063/1.4930861]

I. INTRODUCTION

Metal-insulator transitions (MIT)[1–5] are well established and widely observed phenomena in condensed-matter systems. Despite the common behavior corresponding to a huge change in the electric conductivity, there exist different types of MIT which can be distinguished according to the dominating interaction causing the insulating behavior. Metal-insulator transitions in realistic systems are often considered in a one-particle picture to explain the change of conductivity in a material. In situations such as band, Peierls and Anderson insulators, this yields a successful description, but in the case of Mott insulators the electron-electron correlation gives rise to a contribution which is more important than the electron-ion interaction in the localization of the electronic wave function (WF).[6,7] A Mott transition can occur as consequence of a structure change such as the elongation of the interatomic distances of a metallic system, which causes the electrons to be more localized on different atoms and the consequent drop of conductivity. Despite, strictly speaking MIT can be observed in infinite systems only, some of the characteristic elements of this transitions can be investigated also in finite size clusters, such as drastic changes of the energy gap, of the polarizability and of the localization tensor.

In order to describe Mott-transitions a proper description of the correlated WF becomes crucial, which cannot be in general achieved through the first principle methods usually employed for periodic systems such as the Density Functional Theory (DFT).[8–10] A more sophisticated description can be achieved employing wave-function-based post-Hartree-Fock (HF) treatments which allow to approximate the many-body wave function starting from the HF solution, offering the advantage of being systematically improvable. These methods allow to obtain fairly accurate results for small molecules, but their applicability to extended and periodic systems is limited and not trivial in the present-day because of their unfavorable scaling with respect to the system size. Nevertheless, a way to overcome this problem is offered by local correlation methods[11–22] which are based on the short range nature of dynamic electron correlation and exploit a reformulation of the many-body wave function in terms of localized orbitals (LOs).

Among the different wave function-based local approaches the method of increments (MoI), originally proposed by Stoll[23–27] and further developed by other groups[28–33] has gained a particular attention in the last decade. Single-reference MoI calculations on gapped systems are now state of the art and allow a fair description of the correlation energy, but also some applications to metallic materials have shown promising results[34,35] even if the problem in obtaining well localized orbitals yields some limitations to the method. The use of the MoI with multireference (MR) wave functions is instead a novel approach and as shown in the recent work on bulk metals by Voloshina and Paulus[36] it successfully retrieves almost 100% of the correlation energy with large static correlation.

In our previous investigation,[37] we have exploited the quantum chemical version[40–44] of the density matrix renormalization group (DMRG)[45,46] approach to calculate the ground state energy of a model system, i.e., beryllium ring-shaped cluster and explored the use of quantum information theory (QIT)[47–53] to characterize the wave function and thus determine the metal-like and insulator-like characters of a system in different regions of the potential energy surface (PES). In the present paper, we will focus again on the same system exploring the use of the method of increments for closed-shell systems obtaining whole ground state dissociation curves through a multiconfigurational approach that allows to describe the crossing region where single-reference approaches such as CCSD(T)[54–57] fail. DMRG calculations performed according to the procedure described in our previous work will be used as

reference for testing the MoI approximation to the correlation energy.

Even though a model system is considered, we will underline how the use of standard canonical methods become prohibitive because of the high correlation effects involved especially if aiming at the thermodynamic limit. As we will show the MoI formalism used in this work involves only LOs which allows it to use a limited active space despite large systems are involved. We will exploit this tool to calculate the correlation energy of Be_n rings as large as $n = 90$ and extrapolate the behavior at the thermodynamic limit.

This paper is structured as follows: in Section II, we describe the different formalisms of the MoI as applied in this work, with particular focus on the complete active space MoI; in Section III, the problematics in describing the system with canonical wave function methods are underlined and we give the details of our calculations; in Section IV, we focus on the results obtained for the Be_6 ring in order to highlight the accuracy and the advantages of the multiconfigurational MoI in comparison with different methods; we also report and compare the results obtained for larger rings and the behavior at the thermodynamic limit is extrapolated; our conclusions are finally drawn in Section V.

II. THE METHOD OF INCREMENTS

A. General formalism

The method of increments exploits the short range nature of the electronic correlation. Within this approach localized orbitals are used in order to describe the correlation energy E_{corr} as sum of individual contributions coming from the correlation of different parts of the system. LOs located at the same site are then collected in orbital groups, to which we will refer as bodies. In its general formalism which employs single-reference methods such as coupled cluster (CC) or perturbation theory approaches, only the occupied orbitals are localized and are used together with the virtual canonical orbitals to build the correlation space. This way including more and more bodies, one can compute different contributions to the total correlation energy.

Thus within the MoI, the first step is to neglect the correlation among different sites and to independently compute the contributions given by the excitations from each individual body, freezing the rest of the system at the HF level. We define the correlation energy computed with each such a calculation as the 1-body increment ϵ_i for the ith body.

The sum of all 1-body increments gives us just a fraction of E_{corr} typically ranging between 60% and 90% of the total correlation energy achievable through the chosen method. The remaining part of E_{corr} is enclosed in the higher-order increments which consider the correlation among many bodies. The second step in a MoI calculation consists then in including two bodies (i, j) and considering the excitations from both bodies in order to compute the correlation energy ϵ_{ij}. This way one can define the 2-body increment $\Delta\epsilon_{ij}$ as a correction to the sum of the 1-body increments,

$$\Delta\epsilon_{ij} = \epsilon_{ij} - (\epsilon_i + \epsilon_j). \qquad (1)$$

Similar expressions can be defined for higher-order increments. For instance, the 3-body increments are calculated as

$$\Delta\epsilon_{ijk} = \epsilon_{ijk} - (\Delta\epsilon_{ij} + \Delta\epsilon_{jk} + \Delta\epsilon_{ik}) - (\epsilon_i + \epsilon_j + \epsilon_k). \qquad (2)$$

Combining these contributions, one can finally compute the correlation energy

$$E_{corr} = \sum_i \epsilon_i + \sum_{i<j} \Delta\epsilon_{ij} + \sum_{i<j<k} \Delta\epsilon_{ijk} + \cdots. \qquad (3)$$

Of course, the total correlation energy is completely recovered upon inclusion of all increments, but the above expansion (Eq. (3)) can be truncated in most cases at low-order increments, yielding a meaningful fraction of E_{corr}. Indeed, as pointed out above, the electronic correlation is in general short ranged, and the Coulomb repulsion is a two-particle interaction which implies that the increments decrease with the distance between the bodies i and j (r_{ij}) and the order of the increments (1-body, 2-body, etc.), i.e., the following convergence criteria are fulfilled:

$$|\Delta\epsilon_{ij}| > |\Delta\epsilon_{ik}| \quad \text{for} \quad r_{ij} < r_{ik}, \qquad (4)$$

$$|\Delta\epsilon_{ij}| > |\Delta\epsilon_{ijk}| > |\Delta\epsilon_{ijkl}| > \cdots. \qquad (5)$$

The use of localized orbitals in the MoI and the possibility of truncating Eq. (3) are crucial points in making the method a candidate for the application to extended and periodic systems, for which canonical wave function methods are generally prohibitive. Nevertheless, the MoI cannot be universally applied and fails when the required convergence criteria (Eqs. (4) and (5)) do not occur. Moreover, since the increments might have alternating sign, the MoI is not monotonously converging to the full correlation energy.

B. Multiconfigurational and multireference formalism

As recently shown by Voloshina and Paulus,[36] a multireference MoI approach can be successfully used to calculate the cohesive energy of systems with a high static correlation contribution such as bulk metals. In comparison with the single-reference formalism, a different localization pattern is required in this approach. Indeed, besides the occupied orbitals, also the virtual orbitals important for the evaluation of the static correlation have to be localized. This way one can then calculate incremental static correlation contributions to E_{corr} arising from Complete Active Space Self Consistent Field (CAS-SCF)[58] calculations performed within the bodies constituted by occupied and virtual LOs. Hence, during this step, occupied and virtual local HF orbitals of one, two, three, etc. bodies are used as active orbitals, while the remaining occupied HF orbitals are kept frozen. This prevents the delocalization of the active LOs during the optimization procedure. We will refer to this multiconfigurational approach as the complete active space method of increments (CAS-MoI). Once again the CAS-MoI exploits the short-ranged nature of the electron-electron interaction in order to approximate the total static correlation, by constructing multiconfigurational wave functions with LOs only and by optimizing these orbitals.

On top of such a CAS-MoI calculation, a nearly size-extensive MR calculation such as the MR averaged coupled-pair functional (ACPF) can be performed for each term of
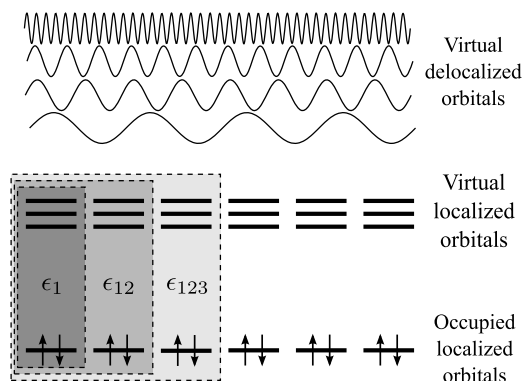
FIG. 1. Sketch of the partition of the active orbitals for the method of increments. In its multireference formalism, CAS-SCF calculations are performed using localized orbitals only as shown in the highlighted boxes in order to obtain the static incremental contributions to the correlation energy. On top of the obtained CAS wave functions, multireference calculations can be performed including excitation to the delocalized virtuals.
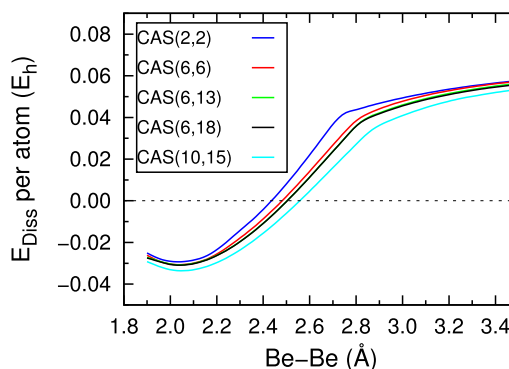

FIG. 2. Dissociation curves calculated for the ground state of Be_{10} at the canonical Complete Active Space Self Consistent Field (CAS-SCF) level of theory, using different active spaces. The dashed line corresponds to the dissociation limit calculated using a CAS(2,4) for the Be atom. A minimal basis set has been used in all cases.

the incremental expansion in order to describe the dynamic correlation. In order to do so, the remaining delocalized virtual orbitals are therefore included to form the active space. This constitutes the final step of the multireference method of increments (MR-MoI). The scheme is sketched in Fig. 1. All equations described in Section II A are used to expand and truncate both the static and the dynamic correlation energies.

Although, the MR-MoI can allow to achieve quantitative results for extended systems which require a multireference description, this goes beyond the aim of this work. We will focus instead on the application of the CAS-MoI to model systems which require very large active spaces for a size-extensive description. We will analyze and discuss the validity of the many-body expansion in dependence of the chosen HF starting configuration used for generating the LOs. Indeed, at this stage, this method still requires a single-reference as a starting point for MoI expansion and in with the aim of describing a whole dissociation curve, the effect of this reference has to be analyzed. As described in Sec. III we will employ a minimal basis set and localize all virtual orbitals which will be used to construct the complete active space for the CAS-MoI calculations. This choice was made because, independently from the LO basis employed, the many-body expansion should converge to the full-CI result, which we can reasonably approximate using DMRG.

III. CALCULATION DETAILS

A. The system

As the subject of our investigation we have chosen beryllium ring-shaped clusters. This model system is characterized by a high static correlation contribution and its pseudo-one dimensional structure resembles the periodic Born-von-Karman boundary conditions. That allows to obtain a WF that will inevitably converge towards the thermodynamic limit of an infinite linear chain as the number of atom is increased. Because of the quasi degeneracy of valence $2s$ and virtual $2p$ orbitals (more than 93% of the correlation energy of the Be atom in its ^1S ground state is static), $4n$ active orbitals

would be required to obtain a size-consistent CAS-SCF reference for multireference calculations for Be_n. This leads to CAS($2n, 4n$) calculations which become of course prohibitive as n increases.

The role of static correlation has been widely investigated for Be_2, for which it is well known that single-reference methods, such as configuration interaction single double (CISD) and CCSD, are unable to give even a qualitative description of the dissociation.[59–64] It was shown that a full valence CAS(4,8) is needed as a start for a consistent multireference calculation. On the other hand, without dynamic correlation, a repulsive curve is obtained for the beryllium dimer showing that a correct balance between static and dynamic correlations is crucial for describing the dissociation of Be_2.

We report in Fig. 2 the dissociation curves of Be_{10} calculated using a minimal atomic basis set and different active spaces within the canonical CAS-SCF method. As one can see, the use of larger and larger active spaces gives a finer and finer description of the potential energy curves, but the calculated dissociation plateaus lie at much higher energies than the dissociation limit calculated within the same method using an active space consisting of the $2s$ and $2p$ functions of the free atom. Similar results are reported in more detail in Table I as described later on.

This model system is even more complicated by the fact that the p functions, besides enlarging the active space, play a significant role already at the Hartree-Fock level. Indeed, in the limit of dissociation the HF orbitals will be linear combinations of pure $2s$ atomic orbitals, while as the interatomic distance shortens their p-character increases until the HOMO switches from a pure s to a pure p molecular orbital. In other words, we encounter a crossing between the two HF configurations which dominate the ground state WF at different interatomic distances. This holds for the finite pseudo-one dimensional clusters independently from their size as well as for the periodic chain given that both the energy and the character of the discrete Hartree-Fock molecular orbitals of Be_n rings converge towards the crystal orbitals. In order to supply a graphical representation of these HF wave functions, we report in Fig. 3 the band structure calculated in the two regimes and the s-character of the Hartree-Fock valence

TABLE I. Comparison between different canonical CAS and RAS approaches, CCSD(T), MRCI(+Q), DMRG calculations performed with a high number of block states according to the procedure described in Ref. 37 and MoI calculation at the 4-body level.

| Calculation	Metal-like – 2.10 Å– Conf 1		Insulator-like – 3.00 Å– Conf 2	
	Energy (E_h)	E_{corr} (%)	Energy (E_h)	E_{corr} (%)
CAS(6,6)	−14.554 946 2	8.07	−14.491 230 8	8.54
CAS(6,12)	−14.560 817 0	29.23	−14.505 672 0	33.55
CAS(6,15)	−14.561 214 2	30.66	−14.505 966 2	34.06
RAS(4,21)	−14.562 199 3	34.21	−14.500 434 7	24.48
CAS(6,21)	−14.562 210 5	34.25	−14.500 464 7	24.53
RAS(6,18)	−14.570 922 5	65.64	−14.524 378 5	65.95
RAS(4,23)	−14.571 467 3	67.60	−14.523 513 7	64.45
RAS(2,24)	−14.575 925 2	83.67	−14.526 707 7	69.99
CCSD(T)	−14.579 871 0	97.89	−14.543 620 5	99.28
RAS(4,24)	−14.579 971 0	98.25	−14.540 037 7	93.08
RAS(6,24)	−14.580 454 5	99.99	−14.543 479 2	99.04
CAS(2,2)+MRCI(+Q)	−14.579 809 7	97.66	−14.542 367 7	97.11
CCSD(T)-MoI(4-body)	−14.579 878 7	97.91	−14.543 617 5	99.28
CAS-MoI(4-body)	−14.579 766 5	97.51	−14.544 030 5	99.99
DMRG(12,24) ($M = 1024$)	−14.580 457 7	100.00	−14.544 010 8	100.00
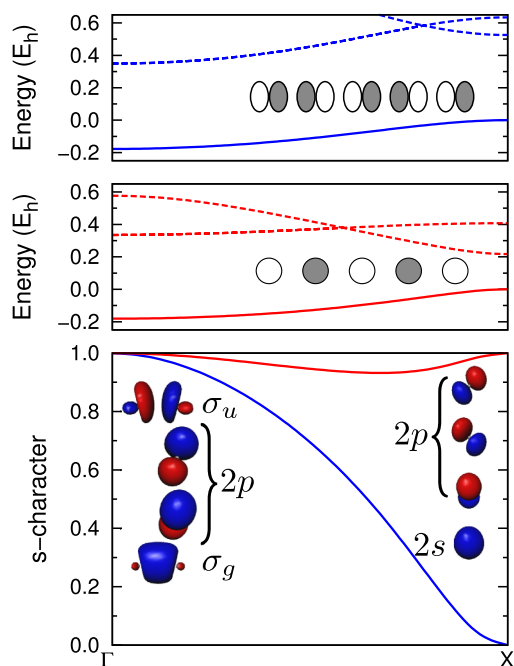
FIG. 3. Hartree-Fock band structure and *s*-character of the valence crystal orbitals of an infinite beryllium chain for the two leading configurations Conf 1 (blue line) and Conf 2 (red line) calculated for interatomic distances of 2.10 Å and 3.00 Å, respectively. The *s*-character, defined as the normalized sum of the squared coefficients of the *s*-bases, is reported in reciprocal space as well as the valence band for the two regimes. Notice that the character of the valence band (full lines) at the X-point of the Brillouin zone switches from pure *p* to pure *s* as sketched in the insets of the upper diagrams. The localized orbitals obtained by unitary transformation of the valence and virtual orbitals are also shown in the lower diagram. As one can see, the difference in *s*-character is reflected by the different symmetry of the localized orbitals.

orbitals of a periodic beryllium chain close to the minimum of the dissociation curve (blue line) and towards dissociation (red line). Respectively, we will refer to these as configuration (Conf) 1 and 2 and we will indicate the two regimes where each of them dominates as metal-like and insulator-like. Clearly a single-reference method such as CCSD(T) will work perfectly in the regimes where one of the configurations is dominant, but not around the crossing region. We will show how the CAS-MoI can allow to overcome this problem even if the WF has a strong multiconfigurational character. This way we will describe the PES of a Be_n ring up to dissociation.

By a unitary transformation of the canonical orbitals of the two main HF configurations different sets of LOs are obtained (see Fig. 3). Indeed, in the insulator-like regime localized orbitals resemble atomic 2*s* and 2*p* orbitals, while in the metallic regime σ_g- and σ_u-like LOs appear. As we will show, the use of the different starting Hartree-Fock configurations has a huge impact on the effectiveness of the method, despite in both cases the result should converge toward the full-CI limit in the chosen minimal basis set.

B. Computation and basis set

The MOLPRO quantum chemistry package[65] was used to perform the different steps of MoI calculations, i.e., Hartree-Fock calculations, Foster-Boys localization,[66] and CAS-SCF calculations. We employed a minimal basis set consisting of 1*s*, 2*s*, and 2*p* atomic functions based on the Dunning *cc*-pVDZ[67] basis set. In particular, we removed the most diffuse *s* and *p* primitive gaussians together with the *d* functions obtaining the contraction $(8s, 3p) \rightarrow [2s, 1p]$ from the original $(9s, 4p, 1d) \rightarrow [3s, 2p, 1d]$. We kept the core 1*s* orbitals frozen during the incremental calculations, focusing on the correlation of valence orbitals. The Crystal09[69] code was employed to calculate the Hartree-Fock wave function of the periodic chain using the same basis set.

IV. RESULTS

A. Be_6 ring

We start our analysis reporting the single-reference CCSD(T) results obtained for Be_6 using both the canonical formalism and the MoI expansion (CCSD(T)-MoI), to illustrate how within the same quantum chemical method, this truncation works in retrieving the correlation energy. The method of increments at the 4-body level retrieves more than the 99.99% of the correlation energy achievable with the canonical CCSD(T) if the proper HF starting configurations (Confs 1 and 2) are used in the two limiting regimes, while around the crossing this percentage drops to around 95%. Also in this regime the $\mathcal{T}_1$ diagnostic calculated within the canonical CCSD(T) presents values larger than 0.03 highlighting the necessity of using a multiconfigurational approach to describe the static correlation. However as already stated and shown in Fig. 2, canonical CAS-SCF approaches cannot be used to calculate a size consistent wave function unless a CAS($2n, 4n$) is performed, i.e., a full-CI in our minimal basis set, and this is of course not applicable as *n* increases. Of course, a
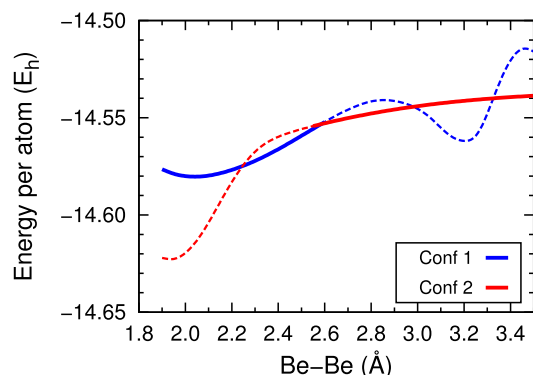
FIG. 4. Energy per atom of a Be_6 ring obtained using the CAS-MoI at the 4-body level starting from the two main HF configurations. The full lines indicate the region where the increments converge with their order yielding results in good agreement with our DMRG reference data. On the other hand, the data indicated by dashed lines show where the MoI approach fails. In the regime between the two dashed vertical lines, both configurations yield proper results.
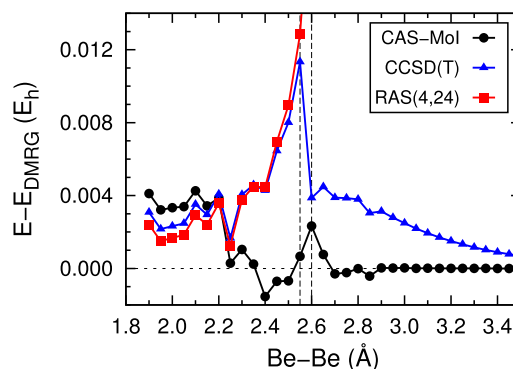

FIG. 5. Comparison between the differences of the PES for Be_6 obtained through different methods (CAS-MoI, canonical CCSD(T) and canonical RAS(4,24)) and DMRG($M = 1024$).

multireference calculation performed on top of an accurate CAS-SCF or RAS-SCF (Restricted Active Space SCF[68]) calculation would reach the required accuracy, but since it is our interest to explore the convergence towards the thermodynamic limit, it is clear that a local method is preferable. Moreover, this choice in general reduces the problem of choosing a proper and consistent active space.

In Fig. 4 we report the total energy curve of Be_6 as obtained using the CAS-MoI at the 4-body level using the Confs 1 and 2. Because in our minimal basis set, the incremental scheme is

converging towards the full-CI solution, it would be in principle equivalent to start from one or the other configuration. However as it can be seen, truncating the correlation energy at the 4-body level the two results match in a narrow regime only, i.e., around the crossing, while for other internuclear distances a non-monotonic behavior is obtained if not the proper HF configuration is used. We want to focus now on the comparison with DMRG data as were obtained as described in our previous investigation[37] with a larger number of block states. As a reference we used results obtained with fixed $M = 1024$ block states and 12 active electrons in 24 active orbitals in order to evaluate the behavior of the CAS-MoI and the other methods discussed. In Fig. 5, we report the absolute error with respect to the DMRG data of the above described
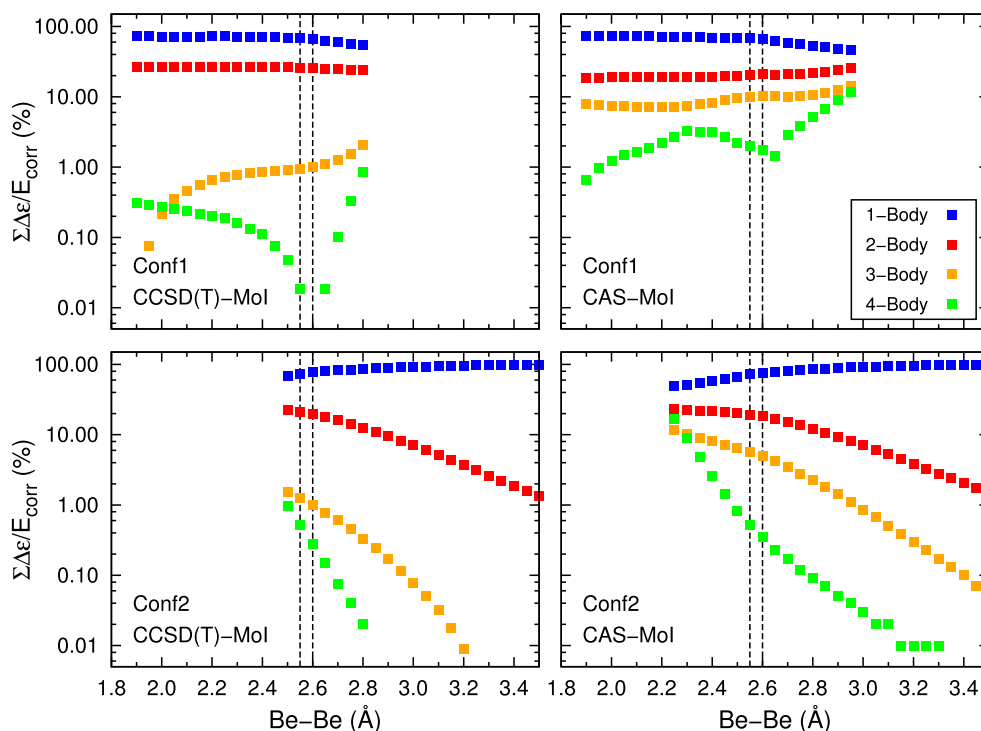

FIG. 6. Percentage of the correlation energy contribution of every incremental order as a function of the interatomic distance for a Be_6 ring obtained with CCSD(T)-MoI and CAS-MoI. The reported data were obtained using configuration 1 (doubly occupied localized σ-like orbitals) and configuration 2 (doubly occupied atomic $2s$-like orbitals) as a starting point for the construction of the localized orbitals. The convergence criteria are fulfilled only in particular distance regimes where the incremental scheme can successfully be used and more than 99% of the correlation energy can be retrieved at the 4-body level. At the crossing point around 2.60 Å, both configurations can be used.
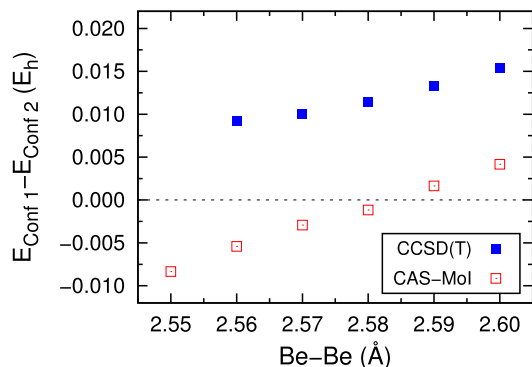
FIG. 7. Difference between the total energy of a Be_6 ring calculated using Conf 1 and Conf 2 as starting configurations. The comparison between the canonical CCSD(T) and the CAS-MoI at the 4-body level is shown around the crossing region. At the full-CI level this difference is expected to be zero.

FIG. 8. Energy difference between CAS-MoI at the 4-body level and DMRG($M = 1024$) for the Be_{10}. In comparison the energy difference between canonical CCSD(T) and DMRG($M = 1024$) is reported.

CAS-MoI, canonical CCSD(T), and the very accurate multi-configurational calculation RAS(4,24) in which up to quadruple excitations were included using all 24 active orbitals. As it can be seen the CAS-MoI gives the best results for almost any interatomic distance, and while the other approaches depart too much from the DMRG reference around the crossing, the CAS-MoI results stay within an error of ± 4 mE_h on the total energy. Looking at the data in Fig. 5, one can notice that for certain interatomic distances, the CAS-MoI yields lower energies than DMRG. This can be explained considering that despite the increments seem to monotonously converge, the missing 5-body and 6-body increments might give small positive contributions to the correlation energy. On the other hand, the maximum value of the truncation error in the reduced density matrix for DMRG calculations ($M = 1024$) within a full sweep was in the range of 10^{-5}–10^{-6}. Therefore the relative error is in the range of 10^{-4}–10^{-5} which leads to an accuracy in the range of 10^{-3}–10^{-4} E_h in the absolute energy.[38,39] Moreover, a larger number of block states or sweeps might retrieve missing amount of the correlation energy. In any case the agreement between the two methods up to 10^{-3} E_h is evident. Only in the metal-like region this approach gives worse results with respect to the other reported even if it underestimates the modulus of E_{corr} only by 2×10^{-3} E_h with respect to RAS(4,24). This can be explained by considering the high delocalization of the wave function in this regime which is hard to describe with a local approach. A quantitative comparison between the results
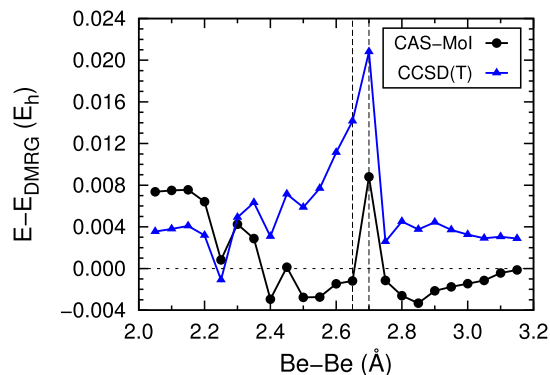
obtained with CAS-MoI, CCSD(T)-MoI, DMRG, CCSD(T) and different CAS and RAS methods is reported in Table I. Again one can realize the difficulty in retrieving a meaningful amount of the correlation energy with canonical methods and how in general the local approach gives reasonable results with less computational effort.

Let us now consider the strong deviations shown in Fig. 4 (dashed lines) that occur when the CAS-MoI is employed starting from a HF configuration which is not the dominant one. In order to explain why in this situation the method fails in describing the electronic structure of the system, let us analyze the behavior of the individual increments as shown in Fig. 6. There can be observed that, as we overcome the crossing, the required convergence criteria stated in Eqs. (4) and (5) break down because higher-order increments give comparable contributions to E_{corr} as lower-order ones. This is equivalent to say that in the employed orbital basis (*i.e.*, HF configuration), higher-order increments become more and more important which is analogous to what was concluded from the analysis of the mutual information as described in our DMRG analysis[37] that showed the increase of the long-range entanglement. This strong dependence on the starting configuration is of course a great disadvantage of the MoI which can otherwise yield accurate results with relatively cheap calculations.

Since we are forced to calculate both configurations, it might appear that no particular advantage arises from the use the CAS-MoI with respect to the single-reference approach. In Fig. 7 we report the differences between the energies

TABLE II. Individual incremental orders, correlation energy per atom E_{corr} and total energy per atom E_{tot} of a Be_6 ring calculated with the MoI at the 4-body level using CCSD(T) (CC-MoI) and CAS-SCF (CAS-MoI).

|	Configuration 1				Configuration 2			
	Metal-like – 2.10 Å		Crossing regime – 2.60 Å		Crossing regime – 2.60 Å		Insulator-like – 3.00 Å	
Increments	CC-MoI	CAS-MoI	CC-MoI	CAS-MoI	CC-MoI	CAS-MoI	CC-MoI	CAS-MoI
ϵ_1	−0.019 707 7	−0.019 508 3	−0.028 255 6	−0.027 883 9	−0.044 322 3	−0.043 834 9	−0.053 221 9	0.053 117 2
$\sum \Delta \epsilon_{1j}$	−0.007 271 9	−0.005 136 4	−0.010 960 4	−0.008 827 9	−0.011 301 6	−0.010 520 5	−0.004 053 9	−0.004 101 3
$\sum \Delta \epsilon_{1jk}$	−0.000 127 6	−0.001 966 6	−0.000 427 2	−0.004 366 2	−0.000 574 5	−0.002 850 8	−0.000 044 7	−0.000 498 5
$\sum \Delta \epsilon_{1jkl}$	−0.000 065 2	−0.000 449 0	−0.000 000 9	−0.000 740 2	−0.000 160 4	−0.000 198 1	0.000 003 5	−0.000 015 7
E_{corr}	−0.027 172 4	−0.027 060 3	−0.039 644 0	−0.041 818 1	−0.056 358 8	−0.057 404 2	−0.057 316 9	−0.057 732 7
E_{tot}	−14.579 878 7	−14.579 766 5	−14.550 047 2	−14.552 221 2	−14.551 826 8	−14.552 872 3	−14.543 617 5	−14.544 033 3
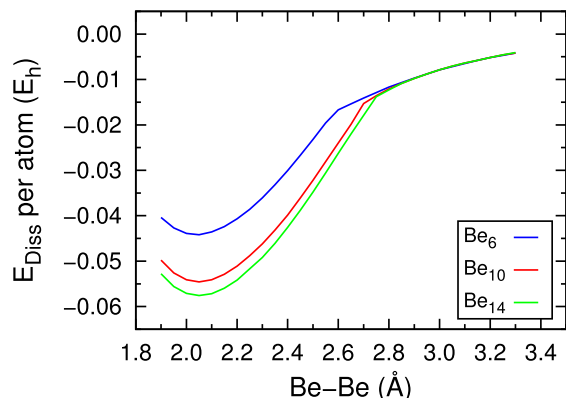
FIG. 9. Potential energy surfaces for Be$_6$, Be$_{10}$, and Be$_{14}$ rings obtained through the CAS-MoI at the 4-body level.

obtained from Conf 1 and Conf 2 in the crossing regime for both methods. As it can be seen, in the case of CAS-MoI this difference is around 10 mE_h smaller than CCSD(T) and ranges between ±5 mE_h. This means that in this narrow regime, the two orbital bases give us comparable results leading to a smooth curve, which is not the case for CCSD(T). In account of this and previous statements, we can conclude that the CAS-MoI allows to describe the behavior of the PES also in the crossing regime allowing us to describe the whole dissociation curve.

We conclude this section comparing the individual increments as obtained from CCSD(T)-MoI and CAS-MoI (see Fig. 6 and Table II). For CCSD(T)-MoI, the lower-increments are larger in magnitude than for CAS-MoI because a larger virtual space is involved, but at the 3- and 4-body levels the orbital optimization which retrieves the static correlation starts

TABLE III. Individual incremental orders and correlation energy per atom calculated with the CAS-MoI for Be$_n$ ring-shaped cluster of different sizes form n = 6 to 90 for two internuclear distances, 2.10 Å and 3.00 Å. The extrapolated values of the correlation energy per atom for the infinite chains are also reported.

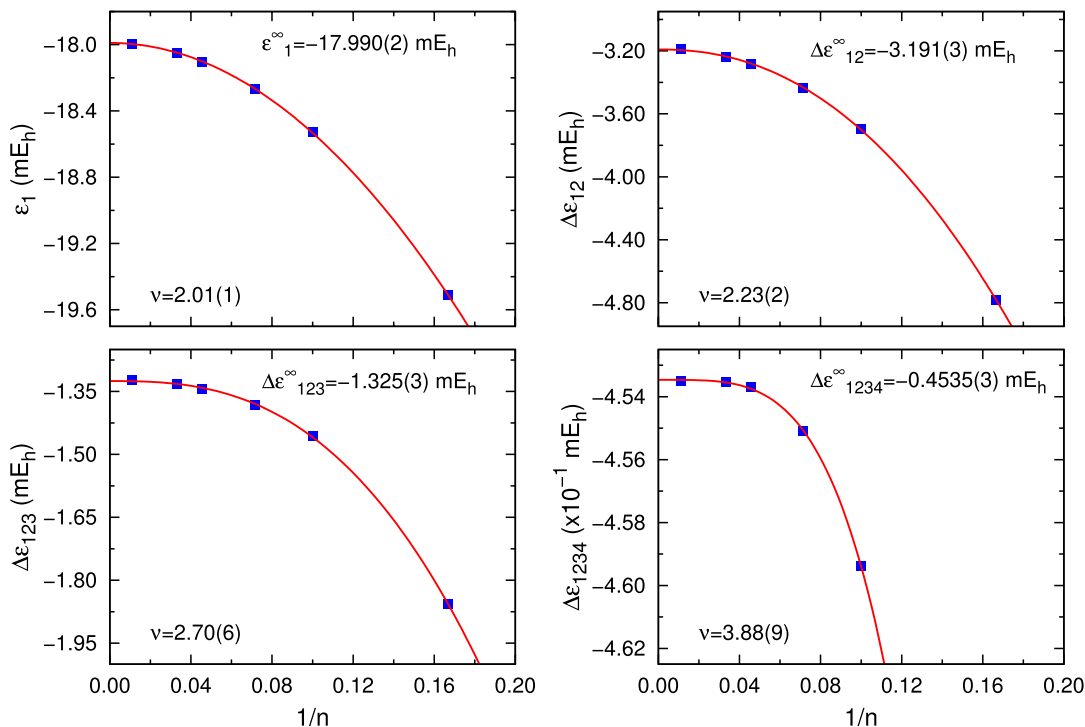|	Metal-like regime – 2.10 Å Conf 1						
Increments	6	10	14	22	30	90	$n \rightarrow \infty$
ϵ_1	−0.019 508 32	−0.018 529 19	−0.018 268 32	−0.018 102 44	−0.018 049 35	−0.017 993 96	−0.017 990(2)
$\sum \Delta \epsilon_{1j}$	−0.005 136 36	−0.003 886 69	−0.003 582 58	−0.003 409 08	−0.003 357 21	−0.003 305 21	−0.003 305(3)
$\sum \Delta \epsilon_{1jk}$	−0.001 966 57	−0.001 527 85	−0.001 457 35	−0.001 418 79	−0.001 407 66	−0.001 396 59	−0.001 402(4)
$\sum \Delta \epsilon_{1jkl}$	−0.000 449 04	−0.000 480 85	−0.000 473 95	−0.000 471 72	−0.000 471 40	−0.000 471 12	−0.000 471 18(4)
E_{corr}	−0.027 060 30	−0.024 424 58	−0.023 782 20	−0.023 402 03	−0.023 285 62	−0.023 166 88	−0.023 155(2)
	Insulator-like regime – 3.00 Å Conf 2						
Increments	6	10	14	22	30	90	$n \rightarrow \infty$
ϵ_1	−0.053 117 19	−0.052 189 30	−0.051 906 79	−0.051 746 49	−0.051 696 82	−0.051 644 40	−0.051 633(7)
$\sum \Delta \epsilon_{1j}$	−0.004 101 30	−0.004 506 50	−0.004 644 82	−0.004 724 04	−0.004 747 99	−0.004 773 69	−0.004 783(6)
$\sum \Delta \epsilon_{1jk}$	−0.000 498 46	−0.000 636 36	−0.000 682 77	−0.000 707 80	−0.000 715 98	−0.000 724 74	−0.000 727(2)
$\sum \Delta \epsilon_{1jkl}$	−0.000 015 74	0.000 021 65	0.000 023 05	0.000 024 33	0.000 024 57	0.000 024 76	0.000 024 7(5)
E_{corr}	−0.057 732 68	−0.057 310 51	−0.057 211 33	−0.057 154 00	−0.057 136 22	−0.057 118 07	−0.057 119(2)
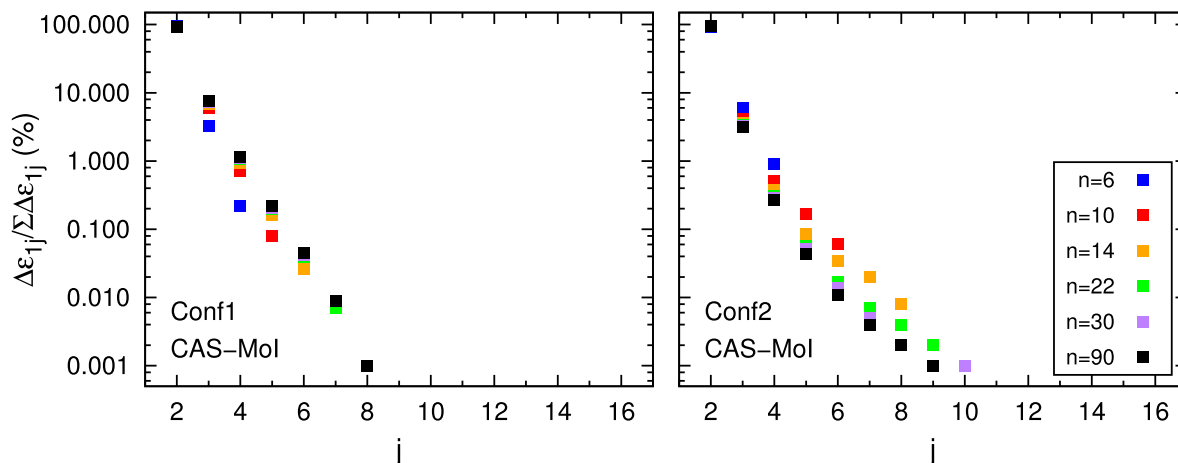
FIG. 10. Percentage given by the individual 2-body increments $\Delta \epsilon_{1j}$ with respect to the total sum of 2-body contributions to the total correlation energy for Be$_n$ rings of different sizes (n ranging from 6 up to 90). The reported data were obtained at internuclear distance 2.10 Å using configuration 1 (doubly occupied localized σ-like orbitals) and at 3.00 Å for configuration 2 (doubly occupied atomic 2s-like orbitals) as a starting point for the construction of the localized orbitals.
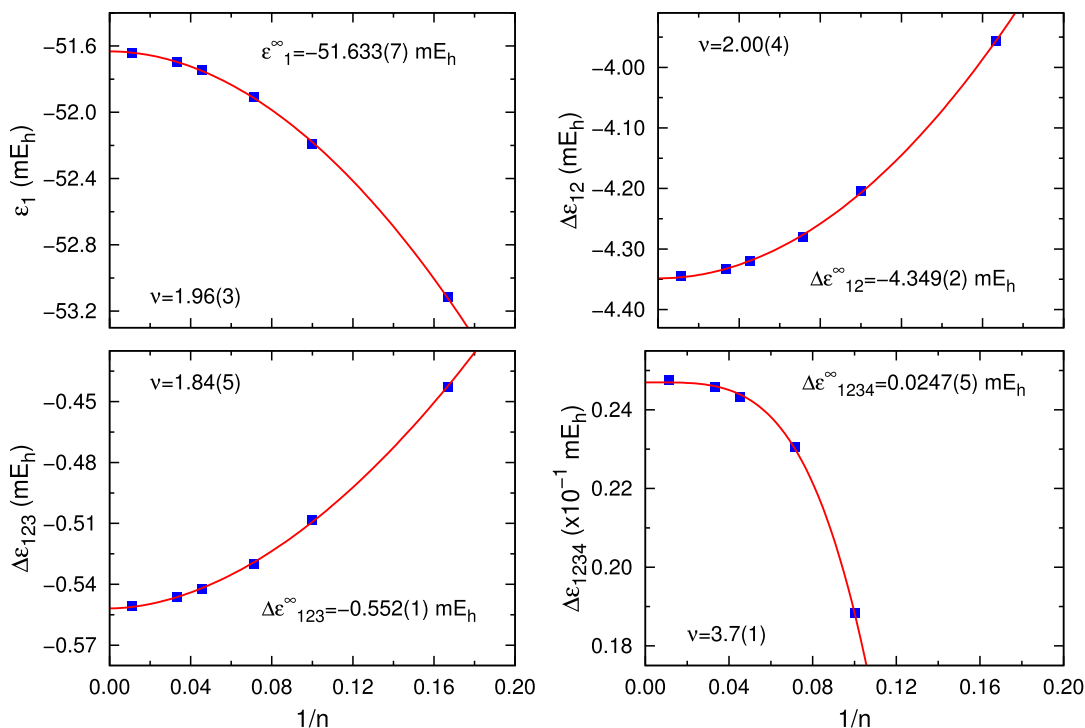
FIG. 11. Convergence with the ring size of the largest individual increments of each order. The red lines were obtained by fitting the calculated data with an equation of the form $a/n^\nu + \varepsilon^\infty$ where ε^∞ is the value extrapolated for the periodic chain.

to play a larger role than the size of the virtual space. In general the single-reference method converges faster, but the total correlation energy is larger in magnitude for CAS-MoI than for the single-reference approach.

B. Extension to larger rings

After analyzing the use of the CAS-MoI for Be_6 we report the results for larger rings in order to evaluate the convergence
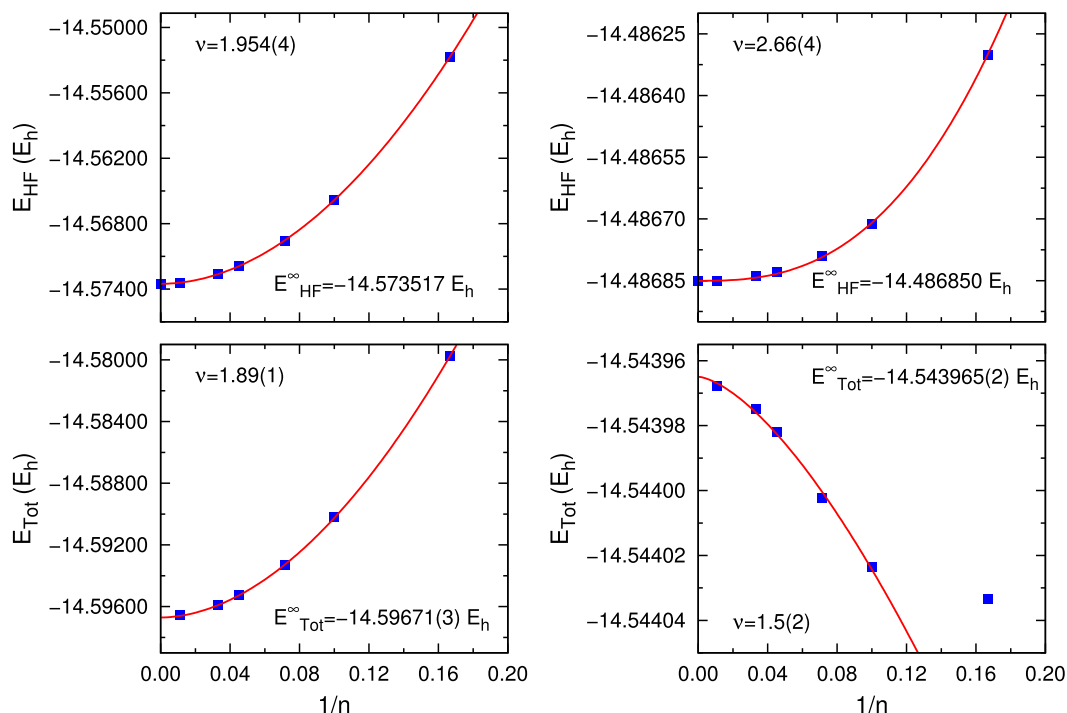
FIG. 12. Convergence with the ring size of the Hartree-Fock and total energy per atom for 2.10 Å (left) and 3.00 Å (right). For the insulator-like case the total energy of Be_6 does not lie on the fitting curve due to the strong curvature in Be_6 rings.

towards the thermodynamic limit. DMRG allowed us to describe the dissociation of a Be_{10} ring (20 electrons in 40 active orbitals) and as for Be_6 we report (Fig. 8) the energy differences of CAS-MoI and canonical CCSD(T) with respect to DMRG. Also in this case it can be seen that the former method behaves much better than the single-reference one and that the obtained values differ from DMRG ones by about 5 mE_h.

As already stated, approaching the aim of describing periodic systems, local methods become better candidates than canonical ones for obtaining accurate correlation energies. Within the CAS-MoI, the number of necessary configuration state functions (CSFs) depends on the order of the increments involved only and not on the size of the system, while in a canonical approach prohibitive active space sizes become necessary. The PES calculated for Be_{10} and Be_{14} rings at the 4-body level are shown in Fig. 9 in comparison with Be_6. Even from these three small clusters we can deduce trends for increasing n, that is, on one hand, a faster convergence in the insulator-like regime than in the metal-like regime and, on the other hand, a shift of the crossing region towards larger internuclear distances.

In order to highlight these convergences we report in Table III the sum of individual incremental orders and the calculated correlation energies for Be_n rings with $n = 6, 10, 14, 22, 30,$ and 90 in the two regimes. Also the contributions given by each 2-body increment to the sum $\sum \Delta \epsilon_{1j}$ are reported in Fig. 10 in order to show how the sum can be truncated without losing significant contributions to the correlation energy. For both configurations and independently from the number of beryllium atoms, summing all terms $\Delta \epsilon_{1j}$ up to $j = 8$ almost 99.999% of the 2-body level contribution to the correlation energy can be retrieved.

As one can see in Fig. 11 the individual increments can be fitted with a $n^{-\nu}$ function. Hence through extrapolation it is possible to evaluate the values for $n \to \infty$, i.e., for the periodic chain, which are also reported in Table III. It can be observed that in both the metal-like and the insulator-like regimes the trend is basically quadratic for the 1-body and 2-body increments while it rapidly deviates for higher-order increments in the metal-like regime where the dependence on the angle is stronger. It has to be underlined that for the 4-body case, the value for $n = 6$ was not included in the fit because it deviates too much from the trend for obvious geometrical reasons. Clearly the 1-body and the 2-body increments dominate the total correlation energy and therefore E_{corr} depends also quadratically on $1/n$. We conclude showing in Fig. 12 that a similar behavior was obtained for the Hartree-Fock and the total energy, too.

Of course a faster convergence would be achieved if linear chains had been considered since no angle dependence would be present as in the ring shaped cluster. However the higher symmetry of the cyclic structure ensures the equivalence of the different bodies and the absence of any boundary effects. Moreover this structure recalls more the periodic Born-von-Karman boundary conditions imposed in the periodic case.

V. CONCLUSION

The method of increments has been applied using the complete active space formalism in order to describe the dissociation of ring shaped beryllium cluster of different sizes. The large static correlation involved in these systems made them good candidates for our analysis. The MoI allowed us to obtain CAS-SCF wave functions that can be further used as basis for

multireference calculations. Key point of this investigation was that we were able to describe the whole PES also where single-reference methods fail, *i.e.*, close to the crossing regime, where the character of the WF changes from metal-like to insulator-like. DMRG calculations previously performed were crucial to evaluate the reliability of our results. The correlation energy of a system as large as Be_{90} was obtained using this approach. We want to underline that within a canonical method this calculation would involve 180 active electrons in 360 active orbitals which without a local approach would be impossible to treat. Finally, investigating different sizes of Be_n rings we could evaluate the correlation energy for the periodic system by extrapolation.

[1] N. F. Mott, Rev. Mod. Phys. **40**, 677–683 (1968).
[2] W. Kohn, Phys. Rev. **133**, A171 (1964).
[3] E. Lieb and F. Wu, Phys. Rev. Lett. **20**, 1445–1448 (1968).
[4] M. Imada, A. Fujimori, and Y. Tokura, Rev. Mod. Phys. **70**, 1039–1263 (1998).
[5] R. Resta, J. Chem. Phys. **124**, 104104 (2006).
[6] F. Gebhard, *The Mott Metal–Insulator Transition: Models and Methods* (Springer, New York, 1997).
[7] N. Mott, *Metal–Insulator Transitions*, 2nd ed. (Taylor & Francis, London, 1990).
[8] R. M. Dreizler and E. K. U. Gross, *Density Functional Theory* (Springer, Berlin, 1990).
[9] H. Eschrig, *The Fundamentals of Density Functional Theory* (B. C. Teubner, Stuttgart, 1996).
[10] W. Kohn and L. J. Sham, Phys. Rev. A **140**, 1133 (1965).
[11] P. Pulay, Chem. Phys. Lett. **100**, 151–154 (1983).
[12] P. Pulay and S. Saebø, Theor. Chim. Acta **69**, 357–368 (1986).
[13] S. Saebo and P. Pulay, Annu. Rev. Phys. Chem. **44**, 213 (1993).
[14] G. Stollhoff and A. Heilingbrunner, Z. Phys. B **83**, 85 (1991).
[15] R. Pardon, J. Gräfenstein, and G. Stollhoff, Phys. Rev. B **51**, 10556–10567 (1995).
[16] K. Kitaura, E. Ikeo, T. Asada, T. Nakano, and M. Uebayasi, Chem. Phys. Lett. **313**, 701 (1999).
[17] M. Schütz, J. Chem. Phys. **113**, 9986 (2000).
[18] M. Schütz and H. J. Werner, J. Chem. Phys. **114**, 661 (2001).
[19] M. Schütz, Phys. Chem. Chem. Phys. **4**, 3941 (2002).
[20] M. Schütz, J. Chem. Phys. **116**, 8772 (2002).
[21] C. Steffen, K. Thomas, U. Huniar, A. Hellweg, O. Rubner, and A. Schroer, J. Comput. Chem. **31**, 2967 (2010).
[22] C. Pisani, M. Schütz, S. Casassa, D. Usvyat, L. Maschio, M. Lorenz, and A. Erba, Phys. Chem. Chem. Phys. **14**, 7615 (2012).
[23] H. Stoll, Chem. Phys. Lett. **191**, 548-552 (1992).
[24] H. Stoll, J. Chem. Phys. **97**, 8449 (1992).
[25] H. Stoll, Phys. Rev. B **46**, 6700-6704 (1992).
[26] H. Stoll, B. Paulus, and P. Fulde, Chem. Phys. Lett. **469**, 90–93 (2009).
[27] H. Stoll, Mol. Phys. **108**, 243–248 (2010).
[28] B. Paulus, Chem. Phys. Lett. **371**, 7–14 (2003).
[29] B. Paulus, Phys. Rep. **428**, 1–52 (2006).
[30] E. Voloshina and B. Paulus, Phys. Rev. **75**, 245117 (2007).
[31] I. Schmitt, K. Fink, and V. Staemmler, Phys. Chem. Chem. Phys. **11**, 11196–11206 (2009).
[32] C. Müller, D. Usvyat, and H. Stoll, Phys. Rev. B **83**, 245136 (2011).
[33] E. Voloshina, Phys. Rev. **85**, 045444 (2012).
[34] B. Paulus, K. Rosciszewski, P. Fulde, and H. Stoll, Phys. Rev. B **68**, 235115 (2003).
[35] W. Alsheimer and B. Paulus, Eur. Phys. J. B **40**, 243–250 (2004).
[36] E. Voloshina and B. Paulus, J. Chem. Theory Comput. **10**, 1698–1706 (2014).
[37] E. Fertitta, B. Paulus, G. Barcza, and Ö. Legeza, Phys. Rev. B **90**, 245129 (2014).
[38] Ö. Legeza and G. Fath, Phys. Rev. B **53**, 14349 (1996).
[39] Ö. Legeza, J. Röder, and B. A. Hess, Phys. Rev. B **67**, 125114 (2003).
[40] G. K.-L. Chan and S. Sharma, Annu. Rev. Phys. Chem. **62**, 465–481 (2011).
[41] K. H. Marti and M. Reiher, Z. Phys. Chem. **224**, 583–599 (2010).
[42] Y. Kurashige, Mol. Phys. **112**, 1485–1494 (2014).
[43] S. Wouters and D. Van Neck, Eur. Phys. J. D **68**, 272 (2014).
[44] S. Szalay, M. Pfeffer, V. Murg, G. Barcza, F. Verstraete, R. Schneider, and Ö. Legeza, Int. J. Quant. Chem. **115**, 1342 (2015).
[45] S. R. White, Phys. Rev. Lett. **69**, 2863–2866 (1992).
[46] S. R. White, Phys. Rev. B **48**, 10345 (1992).
[47] Ö. Legeza and J. Sólyom, Phys. Rev. B **68**, 195116 (2003).
[48] Ö. Legeza and J. Sólyom, Phys. Rev. B **70**, 205118 (2004).
[49] Ö. Legeza and J. Sólyom, Phys. Rev. Lett. **96**, 116401 (2006).
[50] J. Rissler, R. M. Noack, and S. R. White, Chem. Phys. **323**, 519 (2006).
[51] G. Barcza, Ö. Legeza, K. H. Marti, and M. Reiher, Phys. Rev. A **83**, 012508 (2011).
[52] K. Boguslawski, P. Tecmer, Ö. Legeza, and M. Reiher, J. Phys. Chem. Lett. **3**, 3129–3135 (2012).
[53] K. Boguslawski, P. Tecmer, G. Barcza, Ö. Legeza, and M. Reiher, J. Chem. Theory Comput. **9**, 2959-2973 (2013).
[54] F. Coester, Nucl. Phys. **7**, 421 (1958).
[55] F. Coester and H. Kümmel, Nucl. Phys. **17**, 477 (1960).
[56] H. Kümmel, Nucl. Phys. **22**, 177 (1961).
[57] J. Cizek, Adv. Chem. Phys. **14**, 35 (1969).
[58] B. O. Roos and P. R. Taylor, Chem. Phys. **48**, 157–173 (1980).
[59] J. M. Merritt, V. E. Bondybey, and M. C. Heaven, Science **324**, 1548 (2009).
[60] K. Patkowski, R. Podeszwa, and K. Szalewicz, J. Phys. Chem. A **111**, 12822 (2007).
[61] J. Koput, Phys. Chem. Chem. Phys. **13**, 20311 (2011).
[62] X. W. Sheng, X. Y. Kuang, P. Li, and K. T. Tang, Phys. Rev. A **88**, 1 (2013).
[63] W. Helal, S. Evangelisti, T. Leininger, and A. Monari, Chem. Phys. Lett. **568**, 49 (2013).
[64] M. El Khatib, G. L. Bendazzoli, S. Evangelisti, W. Helal, T. Leininger, L. Tenti, and C. Angeli, J. Phys. Chem. A **118**, 6664 (2014).
[65] H. J. Werner, P. J. Knowles, G. Knizia, F. R. Manby, M. Schütz *et al.*, MOLPRO, version 2012.1, a package of *ab initio* programs, 2012, see http://www.molpro.net.
[66] M. Foster and S. F. Boys, Rev. Mod. Phys. **32**, 296 (1960).
[67] B. P. Prascher, D. E. Woon, K. A. Peterson, T. H. Dunning, Jr., and A. K. Wilson, Theor. Chem. Acc. **128**, 69–82 (2011).
[68] J. Olsen, B. O. Roos, P. Jørgensen, and H. J. Aa. Jensen, J. Chem. Phys. **89**, 2185 (1988).
[69] R. Dovesi, V. R. Saunders, C. Roetti, R. Orlando, C. M. Zicovich-Wilson, F. Pascale, B. Civalleri, K. Doll, N. M. Harrison, I. J. Bush, P. D'Arco, and M. Llunell, *CRYSTAL09 User's Manual* (University of Torino, Torino, 2009).